

3D aggregation of wet fibers

C. PY^{1(a)}, R. BASTIEN¹, J. BICO¹, B. ROMAN¹ and A. BOUDAUD²

¹ *Physique et Mécanique des Milieux Hétérogènes, UMR 7636 CNRS - ESPCI - Paris 6 - Paris 7, 10 rue Vauquelin 75005 Paris, France*

² *Laboratoire de Physique Statistique, UMR 8550 CNRS ENS - 24 rue Lhomond 75005 Paris, France*

received 28 August 2006; accepted in final form 19 December 2006

published online 9 February 2007

PACS 46.32.+x – Static buckling and instability

PACS 47.55.nk – Liquid bridges

PACS 81.16.Dn – Self-assembly

Abstract – Wet fibrous structures such as nanotube carpets or macroscopic brushes tend to self-assemble into bundles when the liquid evaporates. The aggregation process relies on a balance between capillary attraction provided by liquid bridges and restoring torque due to structure stiffness. The final self-organized structure is found to result from a cascade of pairing of smaller bundles into bigger ones. We first describe, both experimentally at a macroscopic scale and theoretically, the case of a single pair of fibers and then generalize this description to more complex 3D assemblies. We finally show the relevance of our results to micro-scale experiments from the literature.

Copyright © EPLA, 2007

Introduction. – Surface tension driven self-assembly of micro-structures has been proposed as a useful tool for elaborating micro-devices at scales where conventional machining is not appropriate [1]. Conversely, the capillary attraction and stiction of wet slender structures may also induce disastrous damages in photoresist patterns [2], microelectromechanical systems [3,4], biomimetic materials [5] and is more dramatically involved in lung airway closure (neonatal respiratory distress syndrome) [6]. At a macroscopic scale, a more innocent consequence is the aggregation of the hairs of a wet dog into clumps. Experiments have been recently conducted with carbon nanotube carpets: when a drop of wetting liquid deposited on the surface evaporates, the tubes assemble into bundles leading to “hut” structures [7–12] or cellular patterns [13–15]. In order to capture the elementary mechanisms of this self-assembly, first studies were conducted with two lamellae [16,17] and then 2D macroscopic brushes composed of evenly spaced lamellae [16]. Here we focus on the 3D case which is more relevant for practical applications.

Experimental setup. – The experiment consists in immersing a brush of long (approximately 30 cm) parallel flexible fibers (glass and polystyrene, see caption of fig. 4), clamped in a regular triangular lattice of spacing $d = 3.1$ mm, into a perfectly wetting liquid (silicon oil with

surface tension $\gamma = 20.6 \cdot 10^{-3} \text{ Nm}^{-1}$). When the brush is quasi-statically withdrawn (typical velocity 0.5 mm s^{-1}), a complex 3D aggregation cascade is observed: fibers stick together, forming successively larger and larger bundles (fig. 1). We explore the internal structure of the cascade by scanning successive sections of the brush lit by a horizontal laser sheet. Tracking the position of each fiber as a function of the distance from the roots provides a 3D mapping of the brush. The sticking events are found to occur mainly by the aggregation of two objects (and not three as one could expect for a triangular lattice), see fig. 2.

Two-fibers sticking. – We will first study the capillary binding of two rods which constitutes the elementary mechanism of aggregation within the brush. Two flexible fibers separated by a distance d are immersed in a liquid, then withdrawn. Capillarity tends to stick the two fibers on the largest possible distance, but this costs a high bending energy near the root, where the fibers are clamped perpendicularly to the base. A balance between capillarity and elasticity thus leads the fibers to stick at a finite distance L_{stick} from their root as in [16] (fig. 3). Experimentally, L_{stick} was found to be proportional to the square root of the spacing d between roots, for fibers with different stiffness, see fig. 4. In the following, we show how to predict this sticking length. On the one hand, bending the two fibers to join at a distance L_{stick} requires an

^(a)Present address: Matière et Systèmes Complexes, UMR 7057 CNRS - Paris 7 - 2 Place Jussieu, 75005 Paris, France.

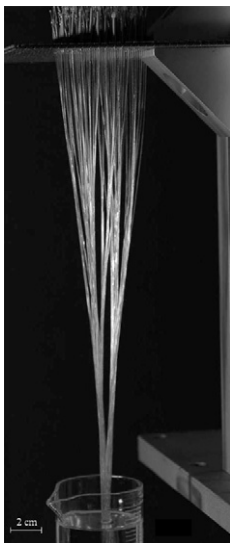


Fig. 1: Brush of fibers withdrawn from a bath of silicon oil. The brush is made of 100 optical fibers with 0.4 mm diameter, spaced by 3.1 mm.

elastic energy

$$E_e = \frac{3EI d^2}{L_{stick}^3}, \quad (1)$$

in the case of small deformation ($d/L_{stick} \ll 1$), where E is Young's modulus and $I = \pi b^4/4$ the area moment of inertia of the fibers with radius b . On the other hand, binding two fibers reduces the liquid-air interface (fig. 3) and thus the surface energy. In the 2D case the surface energy difference is simply proportional to the width of the lamellae [16]. However, in 3D it depends not only on the fibers radius but also on the local shape of the meniscus formed between the two fibers (see fig. 3), and follows [18,19]

$$E_s = \gamma \int_0^{L_{wet}} \left[4b\theta - 4 \left(\frac{\pi}{2} - \theta \right) r \right] dz, \quad (2)$$

where γ is the surface tension of the fluid, and L_{wet} the height of the sticking point above the bath. In the above expression, the first term represents the suppression of the

liquid-air interface in between the fibers and the second term the creation of the two menisci between the fibers. The radius r of the menisci depends on the height z above the liquid free surface through Laplace's law and hydrostatics, $\gamma/r = \rho g z$, whereas the angle θ is geometrically defined by $\cos \theta = b/(b+r) = (1 + \gamma/\rho g z b)^{-1}$. If the saddle shape extremity of the meniscus is neglected, the total energy may be expressed as

$$E = E_e + E_s = \frac{3EI d^2}{L_{stick}^3} - 2\gamma b \int_0^{(L-L_{stick})} \alpha(z) dz, \quad (3)$$

with

$$\alpha(z) = 2\theta - 2 \left(\frac{\pi}{2} - \theta \right) \left(\frac{1}{\cos \theta} - 1 \right). \quad (4)$$

Minimizing the total energy with respect to L_{stick} yields the sticking law,

$$\frac{L_{stick}}{L_{EC}} = \left(\frac{9}{2\alpha} \right)^{1/4} \sqrt{\frac{d}{L_{EC}}}, \quad (5)$$

with α calculated at height L_{wet} , and where L_{EC} is the elasto-capillary length [16] defined as

$$L_{EC} = \left(\frac{EI}{\gamma b} \right)^{1/2}.$$

Therefore in the case of rods, the sticking law depends, through α , on the height L_{wet} above the surface of the liquid. However, in the limit $L_{wet} \ll 2\gamma/\rho g b$ (which corresponds to $\theta \simeq \pi/2$), α is constant and equal to $\pi - 2$. This limit is obviously relevant to micro-structures for which the radius b is very small. Conversely if $L_{wet} \gg 2\gamma/\rho g b$ (which corresponds to $\theta \ll 1$), $\alpha \simeq 2\theta \simeq 2(2\gamma/\rho g b L_{wet})^{1/2}$. This leads to a weak dependence of L_{stick} with L_{wet} , $L_{stick} \sim L_{wet}^{-1/8}$, which is beyond the experimental accuracy. For practical applications, the limit $\alpha = \pi - 2$ is thus relevant for all values of L_{wet} , and L_{stick} may therefore be regarded as independent of the fibers total length. Within this limit, eq. (5) describes very well, and over several decades, the experimental results of the aggregation of two fibers, see fig. 4.

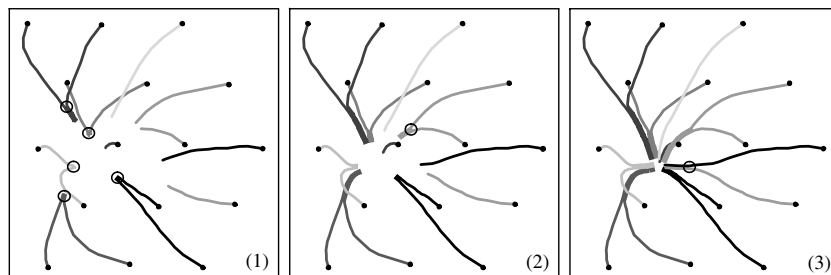


Fig. 2: Top view of the aggregation cascade of a 16-fibers brush at successive heights (15, 14 and 13 cm below the brush's base). Sticking events of two fibers are circled. (1) Couples of fibers stick together. (2) Clumps of pairs of fibers stick together two by two. (3) Final aggregation into a single bundle.

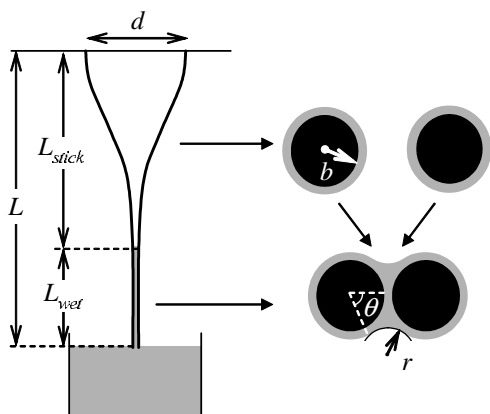


Fig. 3: Sketch of two fibers sticking when withdrawn from a wetting liquid.

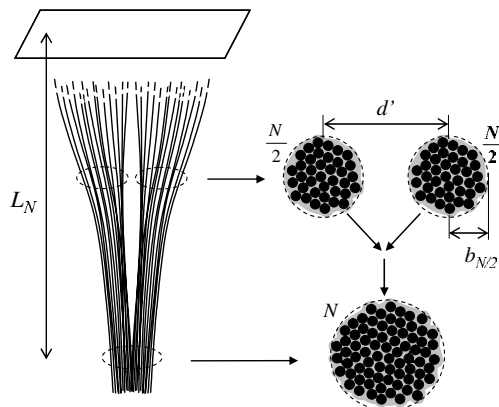


Fig. 5: Aggregation of N fibers resulting from the self-similar clumping of two bundles of size $N/2$.

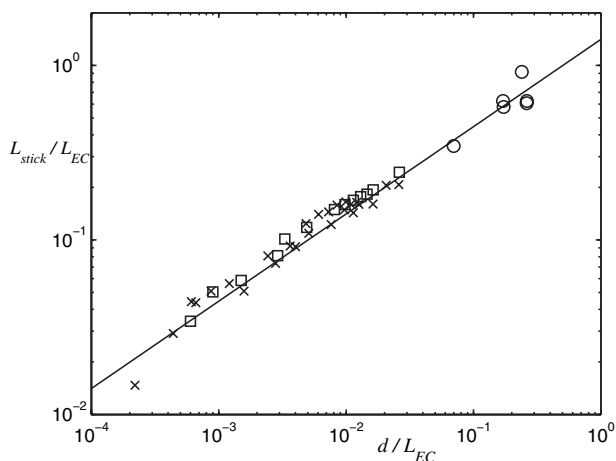


Fig. 4: Sticking distance of two fibers, L_{stick} , vs. root spacing d , for three types of fibers: (o) glass fibers with $L_{EC} = 120$ mm ($EI = 3.1 \cdot 10^{-9}$ Nm 2 , $b = 0.011$ mm, $\gamma = 20.6 \cdot 10^{-3}$ Nm $^{-1}$), (\square) glass fibers with $L_{EC} = 620$ mm ($EI = 5.5 \cdot 10^{-7}$ Nm 2 , $b = 0.07$ mm), (\times) polystyrene fibers with $L_{EC} = 820$ mm ($EI = 2.8 \cdot 10^{-6}$ Nm 2 , $b = 0.2$ mm). (—) Theoretical prediction, eq. (5), with $\alpha = \pi - 2$.

For practical applications [7,13], eq. (5) can be used to estimate the risk of aggregation of rods due to capillarity: if the rods length is smaller than the value of L_{stick} obtained for the considered spacing, collapse will not occur.

Multi-fiber aggregation. – Multi-fiber clusters result from the successive pairing of bundles of increasing size in a self-similar fashion. Let us consider that the aggregation of N fibers results from the sticking of two cylindrical close packed bundles of size $N/2$ (fig. 5). Under this assumption each sub-cluster has a radius $b_{N/2} = b(N\sqrt{3}/\pi)^{1/2}$ and has a global stiffness $N/2 EI$ provided friction between adjacent fibers is neglected. The distance d' between the centers of the sub-clusters before sticking is less trivial to estimate; it scales as $\beta\sqrt{Nd}$, where β is a pre-factor that depends on lattice geometry. The elastic energy

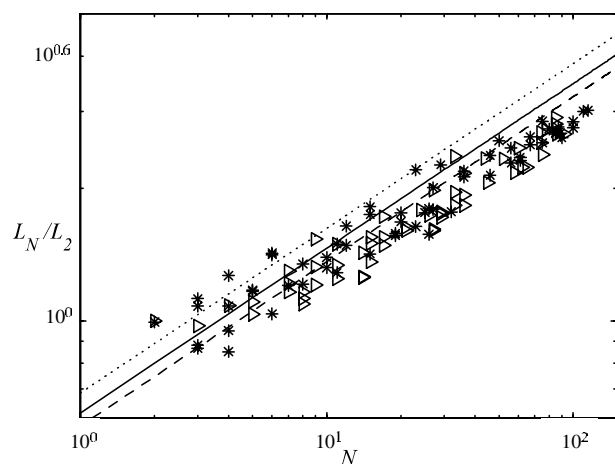


Fig. 6: Sticking length of a 3D brush, L_N , as a function of the number N of fibers involved: optical fibers with $L_{EC} = 820$ mm ($EI = 2.8 \cdot 10^{-6}$ Nm 2 , $b = 0.2$ mm, $\gamma = 20.6 \cdot 10^{-3}$ Nm $^{-1}$) and spacing $d = 3.1$ mm ($*$), $d = 1.9$ mm (\triangleright). Theoretical prediction, eq. (6), with $\beta = 1/\sqrt{2}$ (⋯), $\beta = 1/2$ (---), $\beta = 0.572$ (numerical simulation) (—).

is derived from expression (1) using effective stiffness and spacing of the bundles. The surface energy difference $2\pi\gamma L_{wet}(2b_{N/2} - b_N)$ is slightly different from expression (2) as the bundles rearrange into a bigger cylindrical cluster (fig. 5). Minimizing the total energy with respect to the multi-fiber sticking distance, noted L_N , leads to the following dependence of L_N with N :

$$\frac{L_N}{L_2} = \left(\frac{\beta^2(\pi - 2)}{2\sqrt{\pi} 3^{1/4}(2 - \sqrt{2})} \right)^{1/4} N^{3/8}, \quad (6)$$

where L_2 is the corresponding two-fiber sticking distance given by eq. (5) (with $\alpha = \pi - 2$).

The scaling of the sticking length with $N^{3/8}$ compares well with the experimental results obtained with a large number of brushes of various sizes, and for two different lattice spacings (fig. 6). In practice, the sticking length is difficult to detect by simple imaging when the brush contains many fibers. It was thus measured by

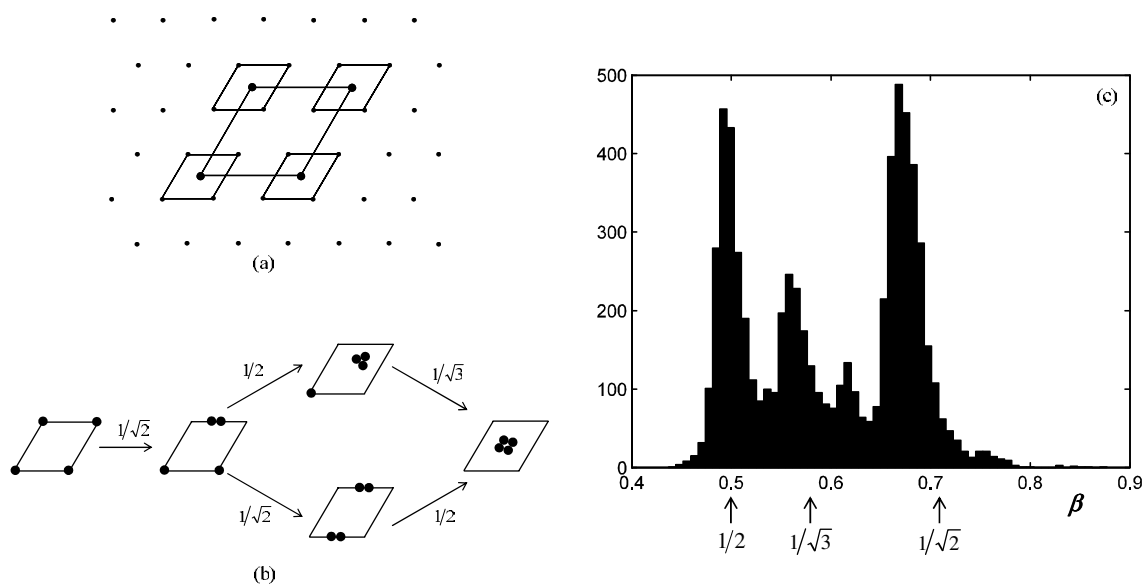


Fig. 7: (a) Rhombus is the repeatable pattern of a triangular lattice. (b) Self-similar sticking scenarios inside a regular lattice with associated β spacing pre-factor at each step. (c) Distribution of the values of β obtained by numerical simulation, and comparison with the three ideal modes shown in (b).

re-immersing slowly the aggregated brush into the liquid until it splits into sub-bundles. The fact that the experimental data seem to follow a slightly smaller slope than the $3/8$ theoretical prediction might be due to finite-size effects¹.

To estimate the spacing pre-factor β we now identify ideal sticking scenarios which preserve the lattice, and thus can be repeated in a self-similar fashion. In such a triangular lattice, the elementary translational pattern is the rhombus, which should be conserved by an ideal cascading process (fig. 7(a)). Two scenarios allow four fibers at the corner of the rhombus to aggregate at its center, see fig. 7(b). For each pairing step, the associated spacing pre-factor β may be identified as $\beta = d'/d\sqrt{N}$, with N the total number of rods sticking together at the considered step. This ideal cascade thus involves several values of beta : β : $1/2$, $1/\sqrt{3}$ and $1/\sqrt{2}$, see fig. 7(b).

To check the relevance of these three ideal modes, we performed a numerical simulation. Some noise was introduced in the location of 6000 points initially set on a regular triangular lattice. Each point is assigned a number N (initially $N=1$) which represents the cluster size. At each step the couple of points with the smallest sticking length (according to the scaling of eq. (6)) is removed and replaced by a summed-up cluster located at the center of mass of the two parents. The spacing between the objects prior to sticking and the associated parameter β is then calculated. The simulation is continued until final

aggregation of all the elements into one unique clump. We obtain the distribution of β shown fig. 7(c), where three main peaks are found close to the three theoretical values. The $1/2$ and $1/\sqrt{2}$ sticking modes are shown to be of larger importance, which is consistent with the fact that they appear in both sticking scenarios. The estimations of the multi-fiber sticking law (eq. (6)) using these two modes compare well with the experimental results, see fig. 6. An additional comparison is made in fig. 6 using the averaged value of β derived from the simulation ($\beta=0.572$), showing also a good agreement.

The multi-fiber sticking law (eq. (6)) also allows to predict, for a given length L of rods, the maximum number of rods that can coalesce due to capillarity. Although a statistical study of the spatial correlations of the bundles within the brush [20], this maximum number gives the typical size of the clusters. The diameter $\xi \sim bN^{1/2}$ of a bundle thus scales as

$$\xi \sim b(L/L_2)^{4/3}. \quad (7)$$

Very similar experiments were performed at nano-scale with carbon nanotube carpets on which a drop of wetting liquid is deposited and evaporates, generating clusters [8]. The average size of these clusters was found proportional to the length of the tube to a power 1.2 ± 0.1 , which is in good agreement with (eq. (7)). Three different theoretical descriptions [8,9,12] have been proposed, leading to the overshooting values $3/2$ and 2 for the exponent².

¹The lack of possible sticking combinations as N increases due to the finite size of our sample leads to an apparent smaller slope for large N . Moreover eq. (6) is correct when the bundles are circular, *i.e.* for large N ; for small N the sticking law should involve a larger prefactor.

²We believe that in [8], the surface energy does not have the right scaling (gravity should not be relevant in this problem), in [12] the capillary rise in between the sticking fibers is not considered and in [9] the spacing between the roots is not taken into account.

Conclusion. – The aggregation of wet fibers clamped on a surface was found to result from a cascade of pairing of smaller bundles into bigger ones. In the case of a single pair of fibers, a balance between capillary forces and elasticity provides a sticking length which scales as $\sqrt{dL_{EC}}$, where d is the distance between the roots and L_{EC} the elasto-capillary length, the lengthscale at which elasticity and capillarity have comparable magnitudes. This relation can be generalized to bigger bundles and leads to a bundle size proportional to $L^{4/3}$, where L is the length of the fibers, which is in good agreement with both macroscopic and microscopic experiments. Although our study focused on a regular triangular lattice, we expect our description to be robust. Different lattices would just result in minor corrections of the pre-factors. The interesting problem of cellular patterns [13–15] remains to be explored. In this case sticking to the ground seems to be important.

We thank DOMINIQUE FONT for encouragement. This work was partially funded by the French ministry of research (Action Concertée Incitative *Structures élastiques minces*), and the Société des Amis de l'ESPCI.

REFERENCES

- [1] SYMS R. R. A., YEATMAN E. M., BRIGHT V. M. and WHITESIDES G. M., *J. Microelectromech. Syst.*, **12** (2003) 387.
- [2] TANAKA T., MORIGANI M. and ATODA N., *Jpn. J. Appl. Phys.*, **32** (1993) 6059.
- [3] MASTRANGELLO C. H. and HSU H. J., *J. Microelectromech. Syst.*, **2** (1993) 33.
- [4] RACCURT O., TARDIF F., ARNAUD D'AVITATYA F. and VAREINE T., *J. Micromech. Microeng.*, **14** (2004) 1083.
- [5] GEIM A. K., DUBONOS S. V., GRIGORIEVA I. V., NOVOSELOV K. S., ZHUKOV A. A. and SHAPOVAL S. Y. U., *Nat. Mater.*, **2** (2003) 461.
- [6] HEIL M. and WHITE J. P., *J. Fluid Mech.*, **462** (2002) 79.
- [7] LAU K. S., BICO J., TEO K. B. K., CHHOWALLA M., AMARATUNGA G. A. J., MILNE W. I., MCKINLEY G. H. and GLEASON K. K., *Nano Lett.*, **3** (2003) 1701.
- [8] ZHAO Y.-P. and FAN J.-G., *App. Phys. Lett.*, **88** (2006) 103123.
- [9] JOURNET C., MOULINET S., YBERT C., PURCELL S. T. and BOCQUET L., *Europhys. Lett.*, **71** (2005) 104.
- [10] NGUYEN C. V., DELZEIT L., CASSEL A. M., LI J., HAN J. and MEYYAPPAN M., *Nano Lett.*, **2** (2002) 1079.
- [11] FAN J.-G., DYER D., ZHANG G. and ZHAO Y.-P., *Nano Lett.*, **4** (2004) 2133.
- [12] FAN J.-G. and ZHAO Y.-P., *Langmuir*, **22** (2006) 3662.
- [13] CHAKRAPANI N., WEI B., CARRILLO A., AJAYAN P. M. and KANE R. S., *Proc. Natl. Acad. Sci. U.S.A.*, **101** (2004) 4009.
- [14] LIU H., LI S., ZHAI J., LI H., ZHENG Q., JIANG L. and ZHU D., *Angew. Chem. Int. Ed.*, **43** (2004) 1146.
- [15] CORREA-DUARTE M. A., WAGNER N., ROJAS-CHAPANA J., MORSCZECK C., THIE M. and GIERSIG M., *Nano Lett.*, **4** (2004) 2233.
- [16] BICO J., ROMAN B., MOULIN L. and BOUDAUD A., *Nature*, **432** (2004) 690.
- [17] KIM H. Y. and MAHADEVAN L., *J. Fluid Mech.*, **548** (2006) 141.
- [18] PRINCEN H. M., *J. Colloid Interface Sci.*, **30** (1969) 69.
- [19] BICO J. and QUÉRÉ D., *J. Colloid Interface Sci.*, **247** (2002) 162.
- [20] BOUDAUD A., ROMAN B. and BICO J., in preparation (2006).